Response of armour rock-scour protection to earthquake-induced liquefaction for offshore wind applications

Diarmid M Xu, C N Abadie, Gopal Madabhushi, John M Harris, Richard J S Whitehouse

ICPMG 2022
10th International Conference on Physical Modelling in Geotechnics
19(Mon) – 23(Fri) September 2022 / KAIST, Daejeon, Korea

Response of armour rock-scour protection to earthquake-induced liquefaction for offshore wind applications

[1]D.M. Xu, [1]C.N. Abadie, [1]S.P.G. Madabhushi, [2]J.M. Harris, and [2]R.J.S. Whitehouse

[1]Department of Engineering, University of Cambridge, Cambridge, UK
[2]HR Wallingford, Wallingford, Oxfordshire, UK

ABSTRACT

Offshore wind is an abundant and indispensable source of renewable energy which recently has seen rapid expansion in East Asia and North America. Soil profiles in East Asia can typically include shallow layers of loose, liquefiable sand overlying competent soil strata which may impact the stability of both the foundation and the scour protection during an earthquake. When employed, scour protection is key to the stability and long-term operation of the wind turbine, and typically consists of graded rocks placed around the foundation to prevent the localised erosion of the soil and any degradation in the foundation behaviour that scour may cause. However, there is limited data currently available on the behaviour of scour protection on liquefiable soils. This paper presents the results of a saturated dynamic centrifuge test that explores the behaviour of large armour rock scour protection on liquefiable soils during seismic events. The use of a combination of sensors and particle image velocimetry enable the recording of rock settlements, accelerations and in particular interstitial pore pressure. The results show that the rock protection prevents the soil beneath it from reaching full liquefaction, but nevertheless, sustains significant settlement during small to medium input motions. The results form the basis for further research into the behaviour of rock protection under dynamic cyclic loading to ensure robust design in seismically active zones.

Keywords: offshore renewable, centrifuge testing, scour protection, seismic loading, particle image velocimetry.

1 INTRODUCTION

Offshore wind is an established but expanding industry that is key to the global energy generation of the future. Worldwide many countries are looking to accelerate significantly their production of offshore wind power, with new developments in seismically active regions such as North America and South Asia. For example, Taiwan is aiming to install 1.5 GW per year, targeting 15 GW by 2035 (Bureau of Energy, Ministry of Economic Affairs, 2021). However, there is very little understanding and experimental data currently available to evidence the behaviour of large-diameter monopile foundations under seismic loads, in particular when installed in liquefiable soils (Seong *et al.*, 2020).

As part of the foundation system, rock scour protection is commonly used to mitigate or remediate scour around the foundation, caused by the erosion of the soil due to the action of waves and currents (Harris *et al.*, 2019). The formation of a scour hole around a monopile foundation will both reduce its capacity and stiffness as the embedded depth is reduced, thus altering the structure's natural frequency. When large scour holes are expected, and mitigation is required, an 8 m diameter pile will have a 30 m diameter × 1.5 m high layer of graded rocks deposited around the monopile to protect against scour. The bottom filter layer typically consists of 0.1 to 0.2 m diameter rocks, poured to a height of approximately 0.5 to 1 m. This is then covered by an armour layer, for example made of 0.5 m rocks, over 1 m in height. Alternatively, a layer of widely graded rocks of ~ 1.5 m thickness can provide both functions.

This method currently remains the most cost-effective choice to remediate scour in offshore wind. Recent developments on scour protection for offshore wind turbines have provided better understanding of the effectiveness of different types of protection and their effect on restoring structural stiffness (Mayall *et al.*, 2020). However, the seismic behaviour of rock scour protection, specifically settlement induced by liquefaction, is not well understood, with limited data currently available in published literature (Escribano *et al.*, 2017). As a result, current design guidelines offer limited or conservative procedures to protect against scour with seismic action (*DNV GL*, 2016, *DNV* 2021).

Notably, the centrifuge tests performed by Escribano *et al.* (2017) show settlements in the region of 0.05 m (Test S02) and a delay to the onset of liquefaction due to the increase in overburden pressure from the presence of the rock berm. This test was performed with 0.5 m diameter armour rocks located on liquefiable loose sand (Table 1).

In this paper, the results of a dynamic centrifuge test are presented, with the aim of comparing to the findings of Escribano *et al*. (2017), and extending the research to incorporate soil displacements below the berm. The centrifuge test, DMX01, contains two models, one with rock, one without. As the sand was poured to fill the entire model box, the only difference between the two sides is the presence of rock, allowing direct comparison. In addition, Particle Image Velocity (PIV) was deployed to capture soil displacements.

2 EXPERIMENTAL METHODOLOGY

2.1 Models design

This paper examines the results of a dynamic test, performed in the 10 m-diameter Turner beam centrifuge at the Schofield Centre (Madabhushi, 2014) at an enhanced gravity of 50 g. Centrifuge modelling enables reduced scale model tests to be performed while preserving stress–strain behaviour of the soil by scaling up the gravity by a factor of N, with N = 50 in this paper. A set of scaling factors relate the model to the prototype response, following Schofield (1980).

The model was prepared in a 730 mm × 250 mm × 400 mm container, with a front acrylic window to enable PIV. A servo hydraulic shaker was used to simulate a series of earthquakes (Madabhushi *et al.*, 2012).

Figure 1 shows model DMX01, with dimensions at prototype scale. The two partitions of the sample were separated by a thin, flexible plastic divider, capable of deforming without adding any additional stiffness to the soil. The divider allowed lateral shaking but was impermeable to the methylcellulose used for saturation of the sample and stopped pore pressure transmission between the two partitions. Figure 2 presents the berm geometry where D_{50} is the rock diameter.

2.2 Rock berm design and model soil

The model rock berm was chosen to represent two layers of poorly graded large 1 m armour rocks with no filter layer in order to test the worst case senario. A mid-range specific gravity for the rock G_s=2.62 was chosen representing standard rather than high density rocks with G_s~3 at this stage.

The sand model was poured in a loose state (relative density = 47 %) with Hostun HN31 sand, d_{50} = 0.44 mm, using an automatic sand pourer (Madabhushi *et al.,* 2006). It was then saturated using methylcellulose, with control over the flowrate during saturation using the "Cam Sat" system (Stringer and Madabhushi, 2009). Table 1 summarises the model properties.

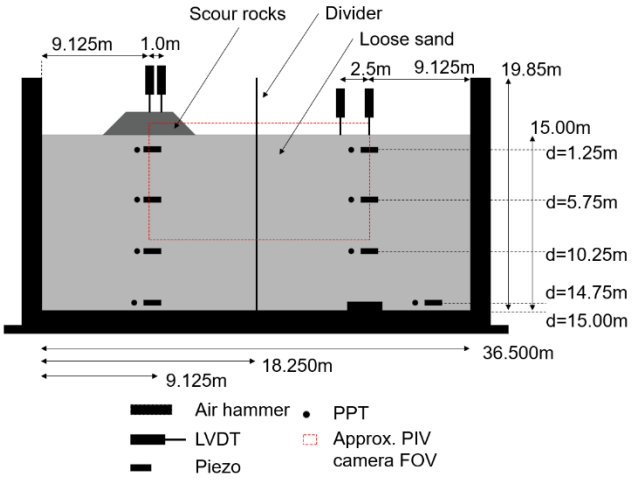

(a)

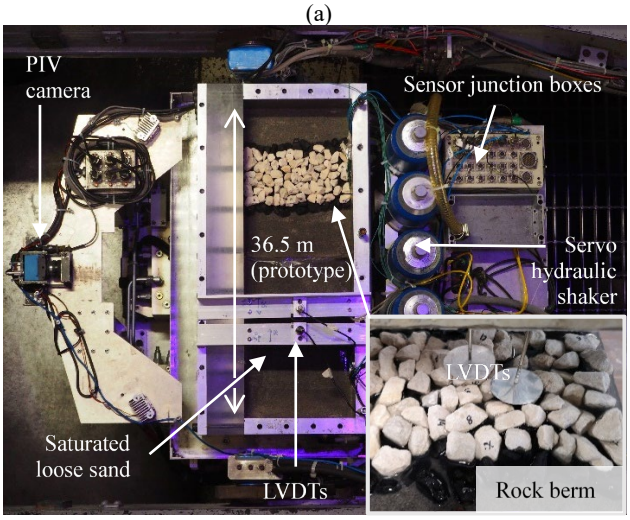

(b)

Fig. 1. (a) Schematic and (b) Photo of test DMX01

Table 1. Armour rock data comparison. (D_{50} is used for scour rock grading, and d_{50} used for sediment grading. t_s is the berm thickness/height.)

Parameter	DMX01 (prototype)	(Escribano and Brennan, 2017)	Field data
d_{50} (mm)	0.44	0.14	0.15
D_{50} (mm)	1000	500	500-1000
t_s (mm)	2000	1500	1500
t_s/D_{50}	2	3	3-1.5
D_{50}/d_{50}	2273	3571	3333-6667
G_s	2.62	-	2.5-3.0

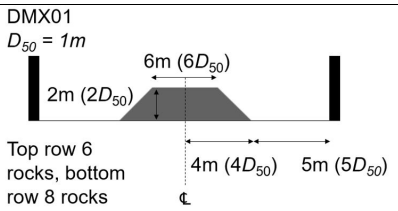

Fig. 2. Berm geometry for DMX01

One of the difficulties in scaling the geometry of rock armour for centrifuge modelling is that respecting the ratio between D_{50}/d_{50} would lead to too fine sand

particles, which are no longer cohesionless. However, reasonable scaling of the rock and sand particles is ensured if D_{50}/d_{50} is greater than 15 (Madabhushi, 2014), which was enforced here at 2273 (Table 1).

The berm geometry was designed with sufficient free sand on either side to allow the sand to flow and heave, thus not obstructing rock settlements. The size of the berm was limited by the size of the model box but was sufficiently large to represent berms in the field.

2.3 Load Sequence

Table 2 presents the earthquake sequences of the test. The voltage input (V) is a measure of the displacement amplitude and hence earthquake strength, with prototype peak bedrock accelerations (i.e. input motion) recorded for plotting. In DMX01, earthquakes of increasing strength were applied with EQ6 lasting for about 10 seconds at field scale.

2.4 Instrumentation

As layers of sand are poured, sensors are placed at selected depths. Pore water pressure transducers (PPT's) and piezoelectric accelerometers are buried in the sand to record pore pressures and accelerations in the sediment at specific locations.

DASYLab v13.0 was used to log data into text files for later processing. A logging rate of 6000 Hz was used for dynamic events, and a rate of 100 Hz was used for swing up, to record pore pressures and settlements as the *g* level increases from one to fifty.

The PIV camera used was the MotionBLITZ EoSens mini 2, model MC 3071. Images were captured at 1696×942 at 900 frames/sec, with a capture time of 1.5 seconds. These images were processed using geoPIV_RG (Stanier *et al.*, 2015).

3 TEST RESULTS

All sensor voltages were filtered, calibrated and zeroed in MATLAB using a bespoke script. An eighth order Butterworth filter was used to reduce phase shift. An approximate initial effective vertical stress has been calculated to identify the limit of liquefaction. For the EQ6 results presented, the selected input motion was a sine wave with an input of 2.5 V, this produced a peak ground acceleration of 0.17*g* (Figure 3).

DMX01 test data contrasts a key finding of (Escribano *et al.*, 2017) comparing the settlements of rock and of free field sand (Figure 3), but confirms that the increase of overburden pressure caused by the presence of the rock berm ensured that the excess pore pressure never exceeded the initial effective vertical stress (i.e. the red dashed line in Figure 4a).

It can be seen that the earthquake produced settlements in the region of 300 mm with a characteristic stop start motion instead of a smooth curve, where the soil stiffens and softens in alternate half cycles to allow

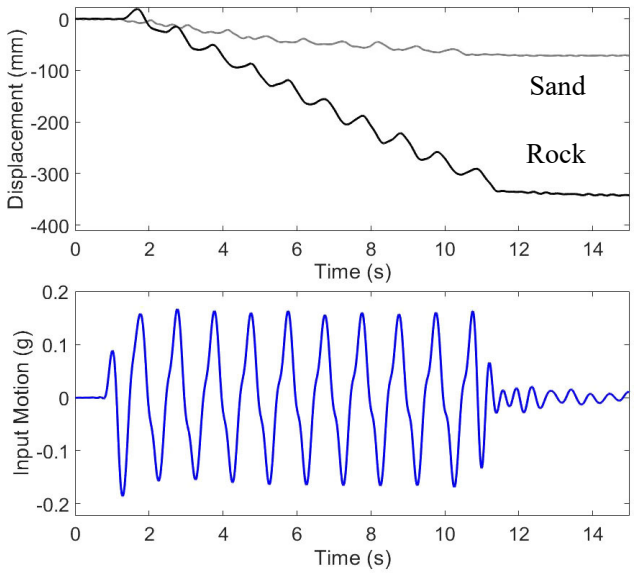

Fig. 3. Settlement of the rock berm in EQ6.

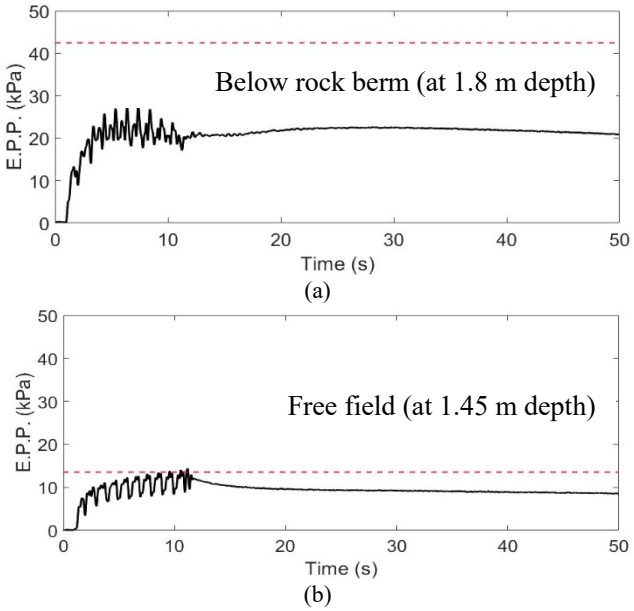

Fig. 4. Comparison of excess pore pressure in (a) below the rock berm and (b) the free-field

Table 2. Earthquake Sequence.

Earthquake	DMX01
EQ1	Sine sweep, 0.7V
EQ2	Kobe, 0.2V
EQ3	Sine wave, 50Hz, 10 cycles, 1.0V
EQ4	Sine wave, 50Hz, 10 cycles, 1.5V
EQ5	Sine wave, 50Hz, 10 cycles, 2.0V
EQ6	Sine wave, 50Hz, 10 cycles, 2.5V

the rocks to sink gradually. Comparing the input motion and LVDT recorded vertical displacements, the results exhibit a delay from the first cycle to the start of settlements. This is because a few earthquake cycles are

required to build up excess pore pressure to partially liquefy the soil.

Figure 4 shows the excess pore pressures for the largest earthquake applied, the red dashed line shows the liquefaction limit. Although excess pore pressures are higher on the rock side, the increase in overburden pressure is far greater. In addition, the data shows that the build-up of excess pore pressure is slower on the rock side, this is because the sinking of rocks causes additional shearing and soil dilation, thus retarding the generation of excess pore pressures. Despite not reaching full liquefaction, these excess pore pressures still caused significant rock settlements.

The results from the PIV displayed in Figure 5 demonstrate that the shallower sediments settle further compared to the deeper sediments under the rock berm. In this figure, a column of data points, 0.5 m to 3.0 m below the mudline is presented for clarity.

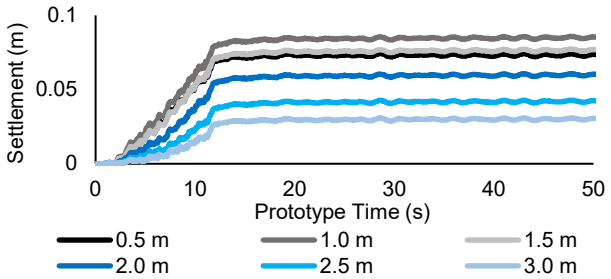

Fig. 5. Comparison of sand settlement below the rock berm.

4 CONCLUSIONS

The data from the centrifuge test has shown that:

1. Rock berm settlements in the region of 300 mm are observed post seismic liquefaction (Figure 3), which is in contrast to the findings of Escribano *et al.* (2017).
2. The presence of rock delays the onset of full liquefaction compared to the free-field sand (Figure 4).
3. Despite not reaching full liquefaction, large settlements still occurred.
4. The PIV technology deployed captures the sand failure mechanism during a dynamic centrifuge test.

These results show that after a significant seismic event, there is indeed the need to inspect rock berms at offshore wind foundations and carry out remediation work as required. Future centrifuge tests are planned to investigate the effect on settlements of the rock size, type, mixed grading and berm geometry.

REFERENCES

Bureau of Energy, Ministry of Economic Affairs (MOEA), July 2021. Offshore Wind Zonal Development: Capacity Raised to 1.5 GW per Year with Flexibility for IRP Options. https://www.moeaboe.gov.tw/ECW/English/news/News.aspx?kind=6&menu_id=958&news_id=19871 (accessed in January 2022)

Chian, S.C., Stringer, M.E., Madabhushi, S.P.G. 2010. Use of automatic sand pourers for loose sand models, in: *Physical Modelling in Geotechnics - Proceedings of the 7th International Conference on Physical Modelling in Geotechnics 2010, ICPMG 2010*. CRC Press, pp. 117–121.

Department for Transport and Foreign, Commonwealth & Development Office, 2021. Decarbonising Maritime Operations in North Sea Offshore Wind O&M.. Available at: https://www.gov.uk/government/publications/decarbonising-offshore-wind-operations-and-maintenance-roadmap (accessed January 2022)

Escribano, D. and Brennan, A. 2017. Stability of scour protection due to earthquake-induced liquefaction: Centrifuge modelling. *Coastal Engineering*, 129, pp. 50–58.

Harris, J.M. and Whitehouse, R. 2017. Scour Development around Large-Diameter Monopiles in Cohesive Soils: Evidence from the Field. *Journal of Waterway, Port, Coastal, and Ocean Engineering*, 143(5), p. 4017022.

Harris, J.M. et al. 2019. Foundation Scour as a Geohazard. *Journal of Waterway, Port, Coastal, and Ocean Engineering*, 145(6), p. 4019022.

Madabhushi, S.P.G., Houghton, N.E., Haigh, S.K. 2006. A new automatic sand pourer for model preparation at University of Cambridge, in: *Physical Modelling in Geotechnics, 6th ICPMG'06 - Proceedings of the 6th International Conference on Physical Modelling in Geotechnics*. pp. 217–222.

Madabhushi, G.S.P. et al. 2012. Development of a servo-hydraulic earthquake actuator for the Cambridge Turner beam centrifuge. International Journal of Physical Modelling in Geotechnics, 12(2), pp. 77–88.

Madabhushi, G.S.P. 2014. *Centrifuge Modelling for Civil Engineers*, *Centrifuge Modelling for Civil Engineers*. doi: 10.1201/9781315272863.

Mayall, R. et al. 2020. Flume tank testing of offshore wind turbine dynamics with foundation scour and scour protection. Journal of Waterway, Port, Coastal, and Ocean Engineering, 146(5), p. 4020033.

Schofield, A.N. 1980. Cambridge Geotechnical Centrifuge Operations. Géotechnique, 30(3), pp. 227–268.

Seong, J., Abadie, C.N., Haigh, S.K. & Madabhushi, G.S.P. 2020. Seismic response of offshore wind monopiles in cohesionless soils. *4th International Symposium on Frontiers in Offshore Geotechnics 2020.* ISFOG 2020, pp. 2137-2146.

Stringer, M.E. and Madabhushi, S.P.G. 2009. Novel Computer-Controlled Saturation of Dynamic Centrifuge Models Using High Viscosity Fluids. *Geotechnical Testing Journal - GEOTECH TESTING J*, 32.

Standard DNVGL-ST-0126. 2016. Available at: https://rules.dnv.com/docs/pdf/DNV/ST/2016-04/DNVGL-ST-0126.pdf.

Standard DNVGL-RP-0585. 2021. Available at: https://www.dnv.com/energy/standards-guidelines/dnv-rp-0585-seismic-design-of-wind-power-plants.html.

Stanier, S. *et al.* 2015. Improved image-based deformation measurement for geotechnical applications, *Canadian Geotechnical Journal*. doi: 10.1139/cgj-2015-0253.

Zhao, Y. et al. 2006. Calibration and use of a new automatic sand pourer', in *Physical Modelling in Geotechnics, 6th ICPMG'06 - Proceedings of the 6th International Conference on Physical Modelling in Geotechnics*. CRC Press, pp. 265–270.